Comparative study of GNSS phase scintillation and high latitude electrodynamic ionospheric properties derived from AMPERE

Robert Robinson (The Catholic University of America)
Jun Wang (Colorado State University)
Jade Morton (Colorado State University)
Ja Soon Shim (The Catholic University of America)
James Secan (NorthWest Research Associates)

AMPERE Measurements of Field-Aligned Currents

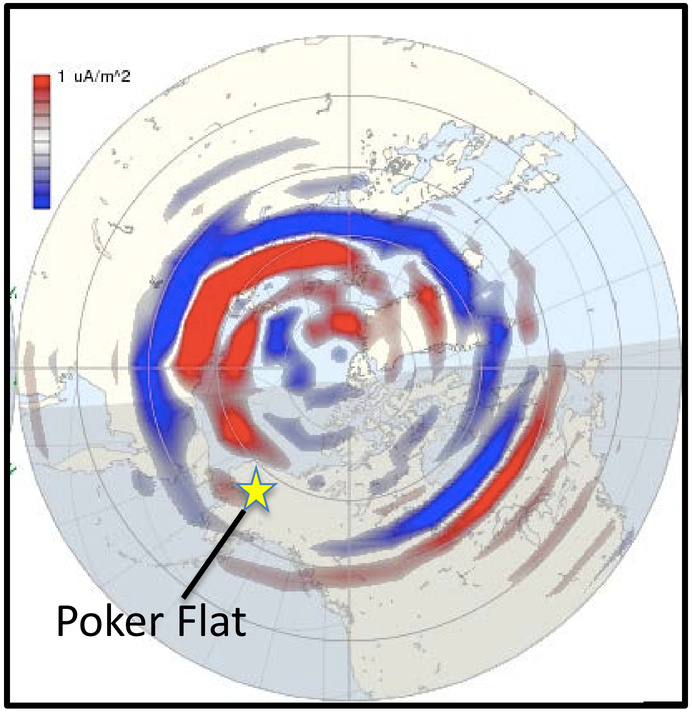

+

Poker Flat Incoherent Scatter Radar measurements of ionospheric electron densities

Measurements every 10 minutes
18 geomagnetically active days

2592 simultaneous and coincident measurements of height-integrated ionosphere conductivities and field-aligned currents

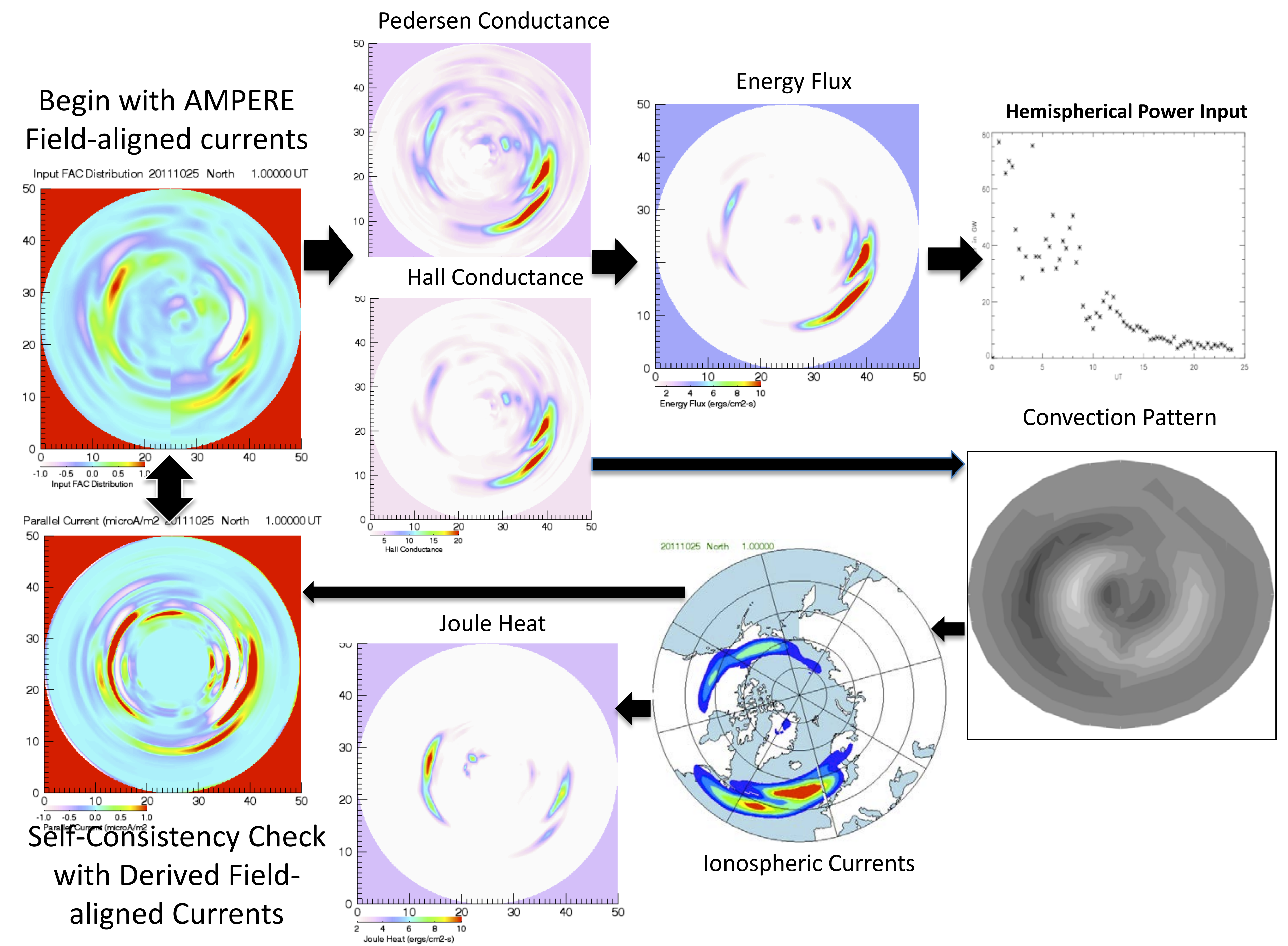

Begin with AMPERE Field-aligned currents
Input FAC Distribution 20111025 North 1.00000 UT
Input FAC Distribution
Pedersen Conductance
Hall Conductance
Hall Conductance
Energy Flux
Energy Flux (ergs/cm2-s)
Hemispherical Power Input
UT
Convection Pattern
20111025 North 1.00000
Ionospheric Currents
Joule Heat
Joule Heat (ergs/cm2-s)
Parallel Current (microA/m2 20111025 North 1.00000 UT
Parallel Current (microA/m2
Self-Consistency Check with Derived Field-aligned Currents

AMPERE-Derived Space Weather Products

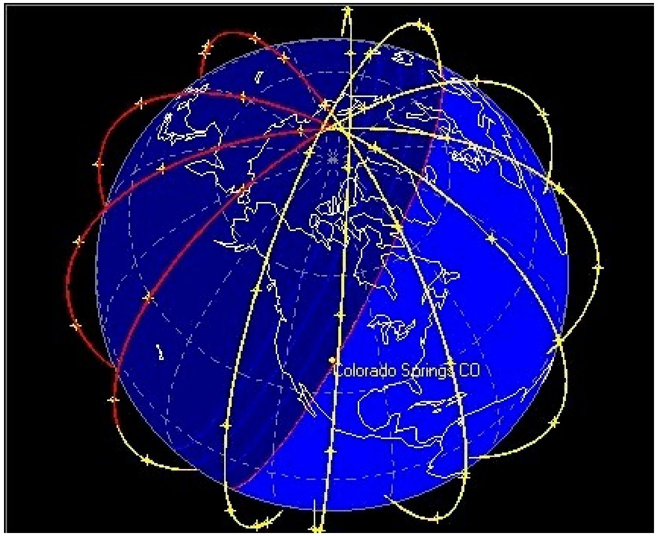

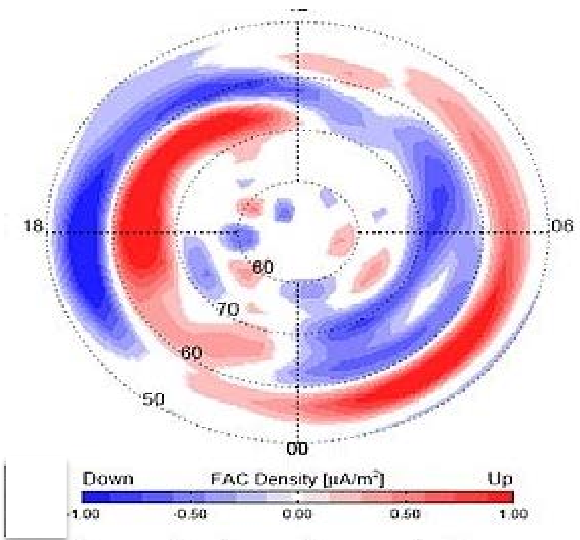

- Aurorally-produced conductivities
- Local and hemispherically integrated auroral energy flux
- Cross Polar Cap Potential
- High latitude electric fields and currents
- Joule heating
- Ground magnetic perturbations
- Auroral electron density profiles to 250 km altitude
- Line-of-sight electron density and total electron content

AMPERE Electrodynamics Validation Studies

- Hemispheric Power Input—OvationPRIME
- Single-site high latitude ground-magnetic perturbations
- 12-station AE index
- Study of six substorms at Poker Flat, Alaska
- Localized energy flux comparison with ground-based optically-derived values
- Global energy deposition comparison with GUVI and SSUSI optical imagery
- Global energy deposition from precipitation and Joule heating comparison with Dst and Sym-H
- High latitude convection comparison with PFISR and GNSS phase error measurements
- Velocity shears related to high latitude scintillation
- Energetic particle precipitation compared with Polar Mesospheric Summer Echo Occurrence rates at Eureka
- Global energy deposition compared with MMS observations
- Energy deposition from precipitating particles comparison with VAP and balloon-based REP measurements
- Global energy deposition compared with ground-based TEC measurements
- High latitude currents compared with SWARM observations

GNSS System Setup

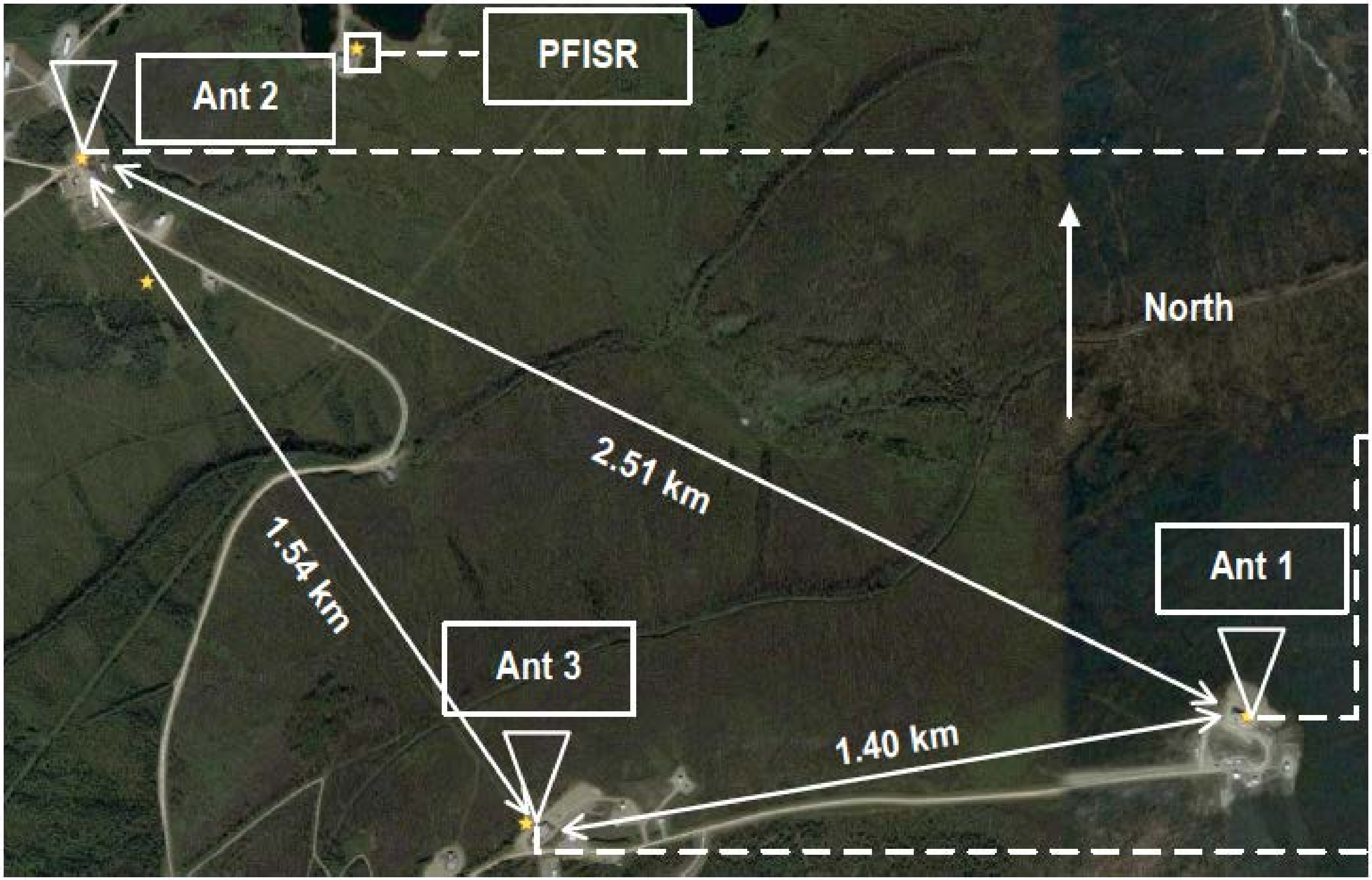

Ant 2
Septentrio PolaRxS GPS/GLO/ GAL/BEI

Ant 1
Septentrio PolaRxS GPS/GLO/ GAL/BEI RF front end

Ant 3
Septentrio PolaRxS GPS/GLO/ GAL/BEI

Correlation Btw Geomagnetic Field Disturbance and GNSS Measurement Error Indicators

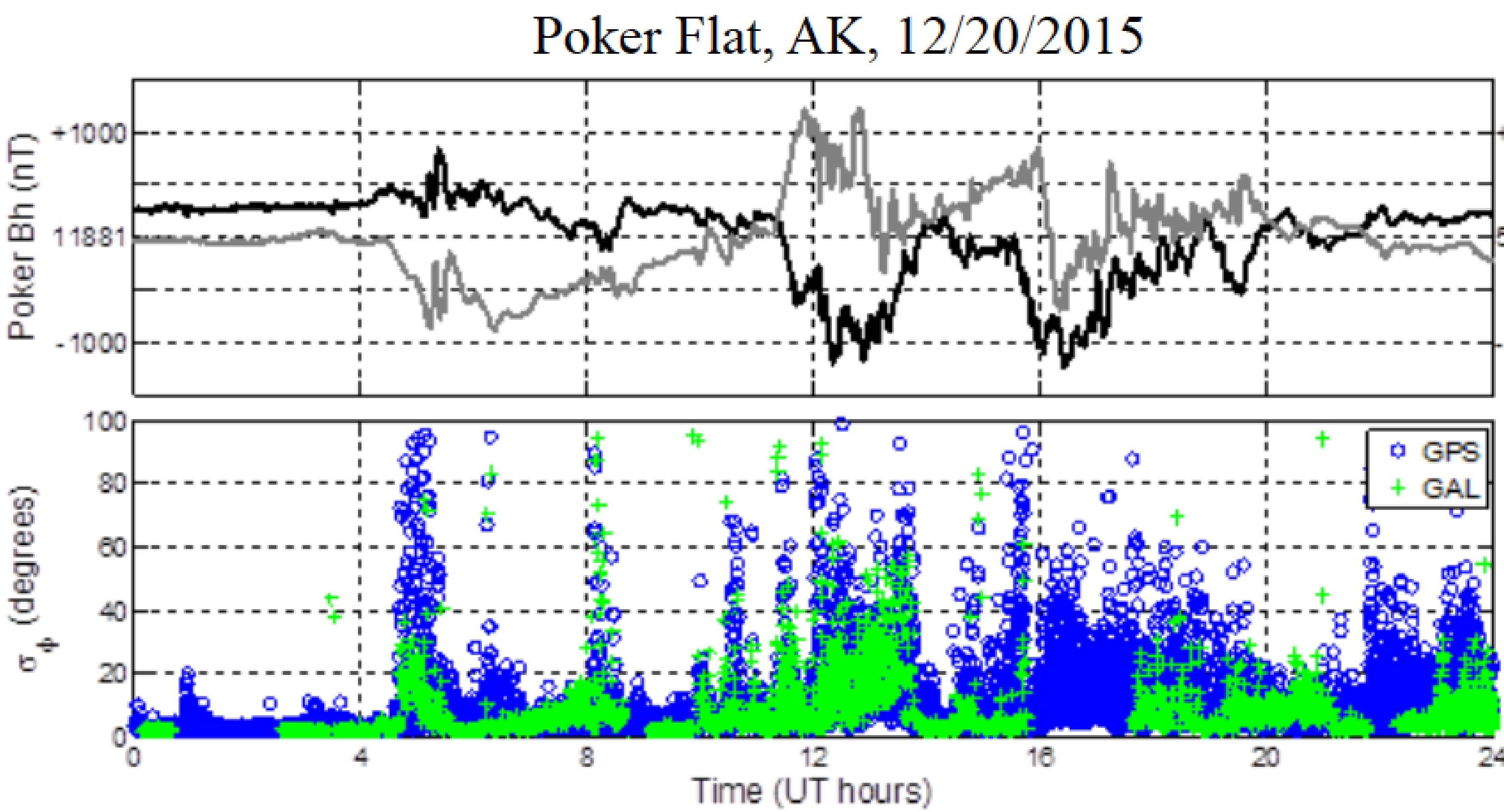

20151231 North   12.0000

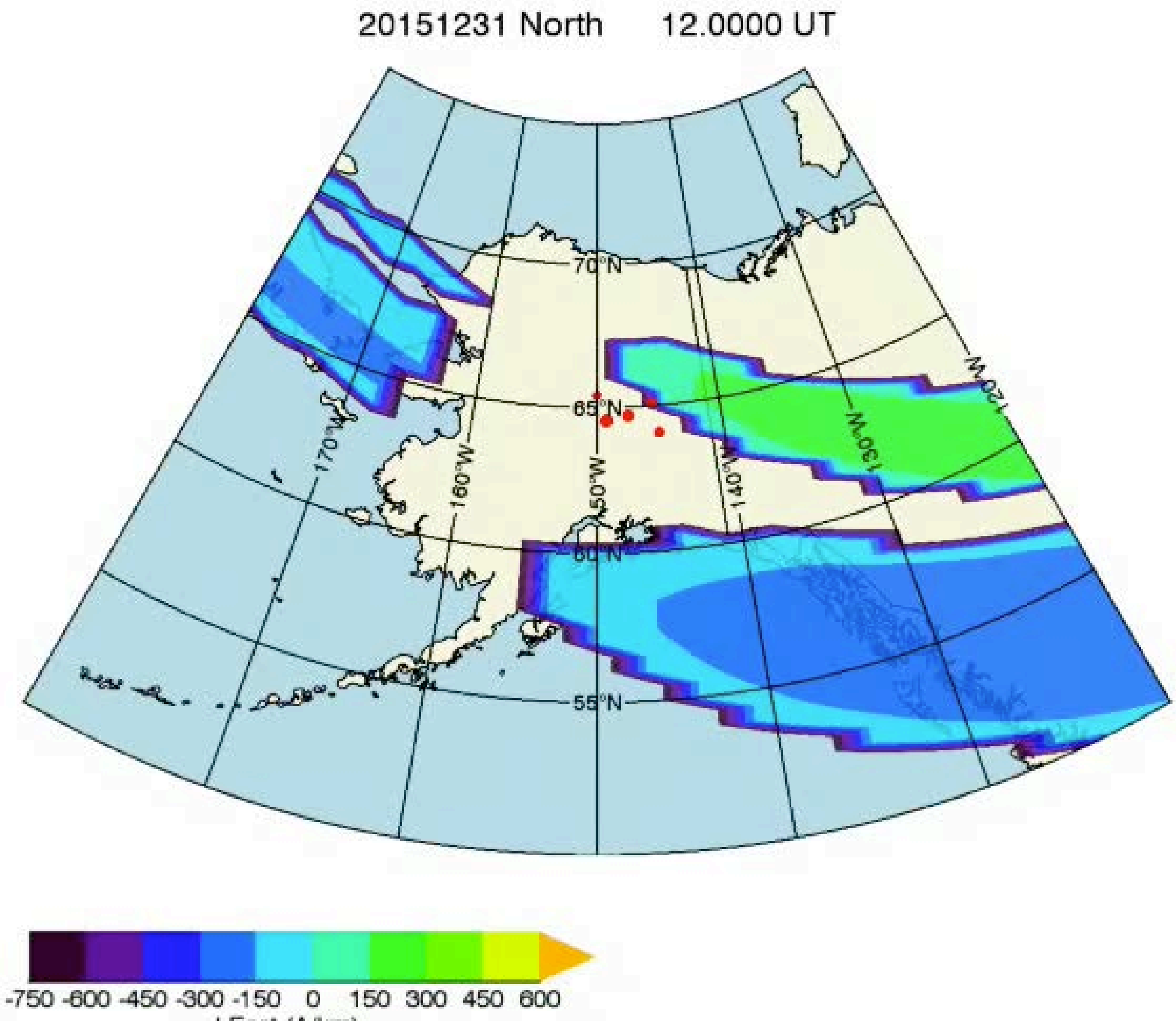

December 20, 2015 GNSS phase compared to E-north times shear in E-north

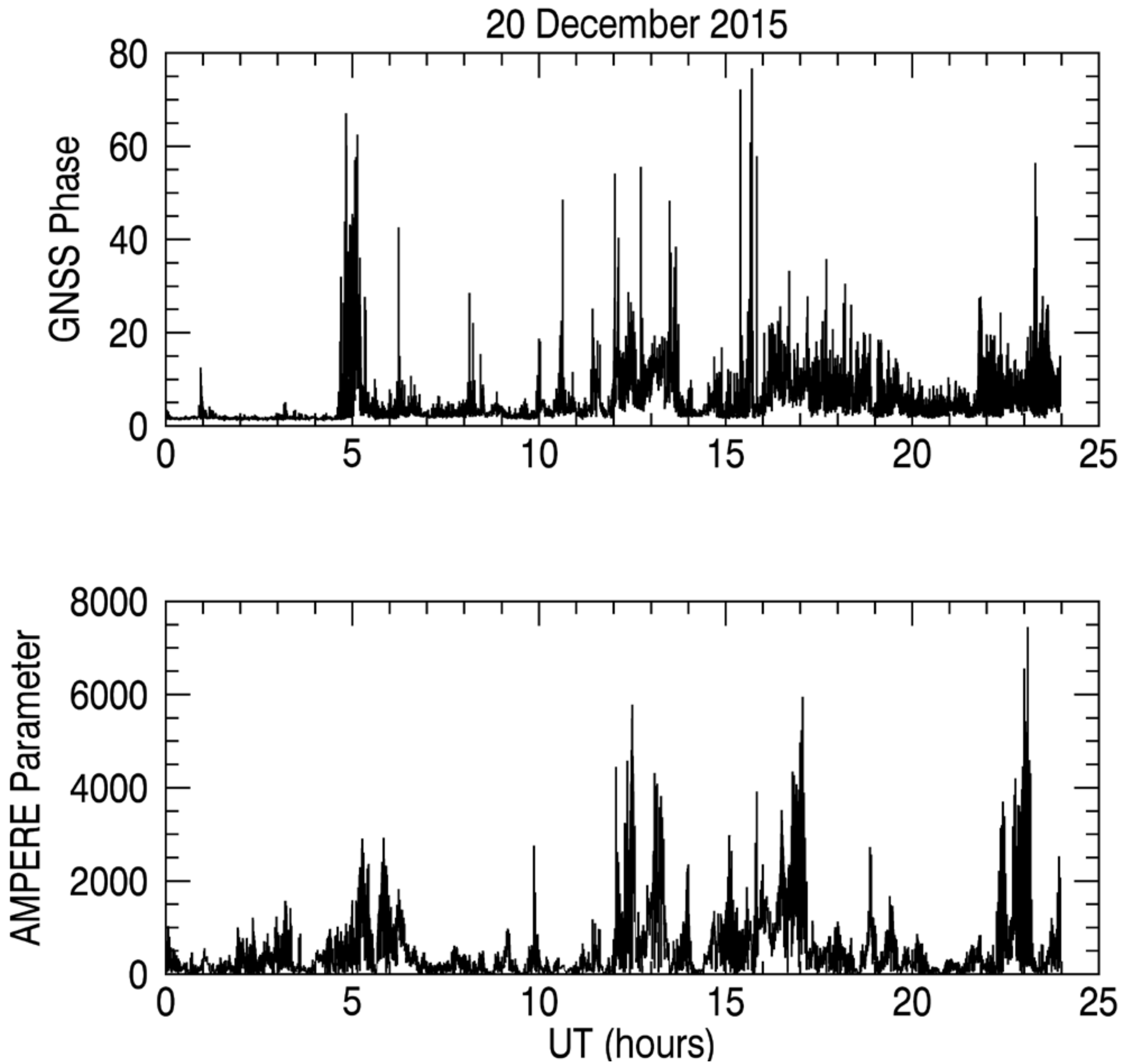

December 20, 2015 GNSS phase compared to E-north times shear in E-north

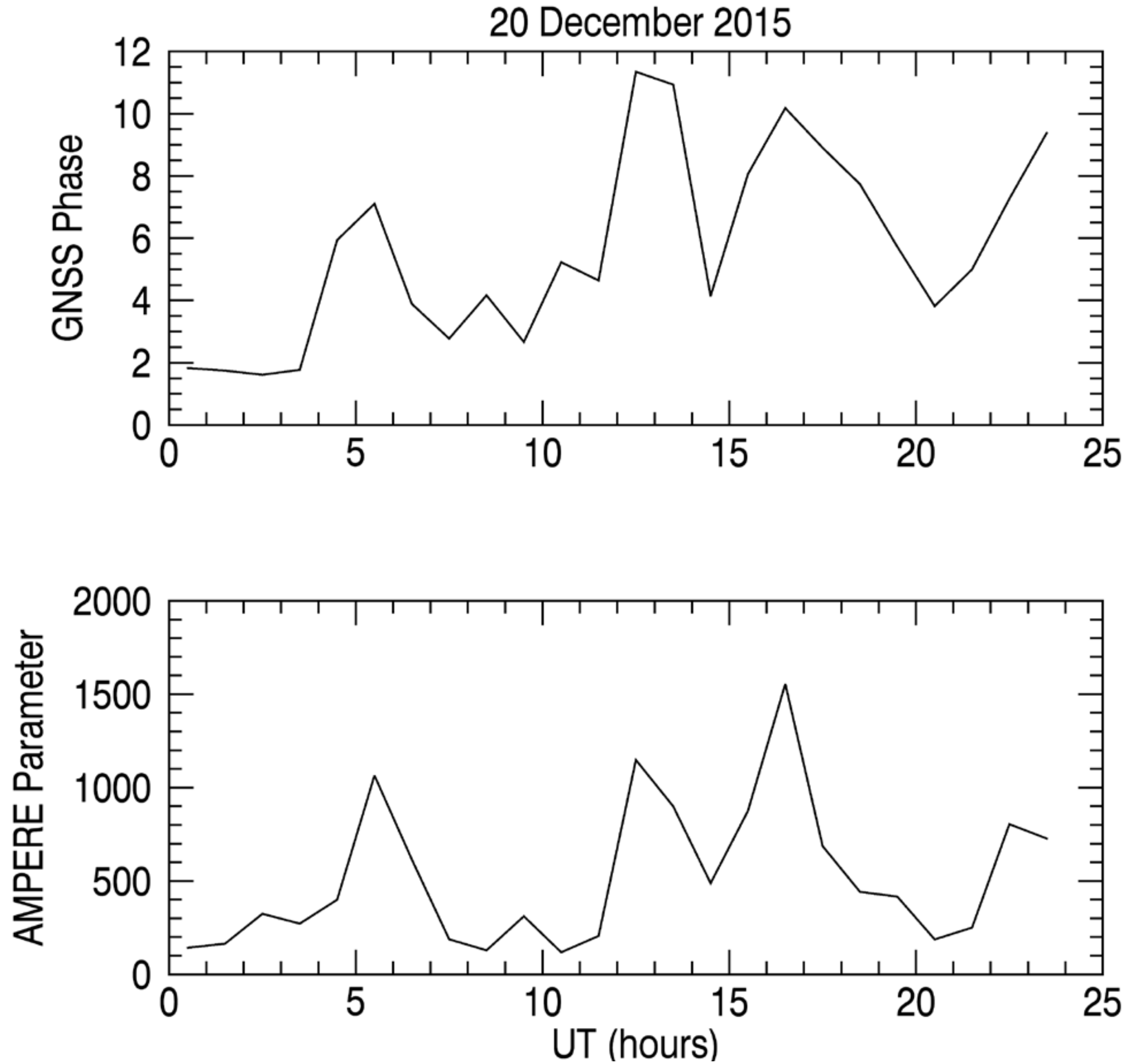

December 20, 2015 GNSS phase compared to E-north times shear in E-north

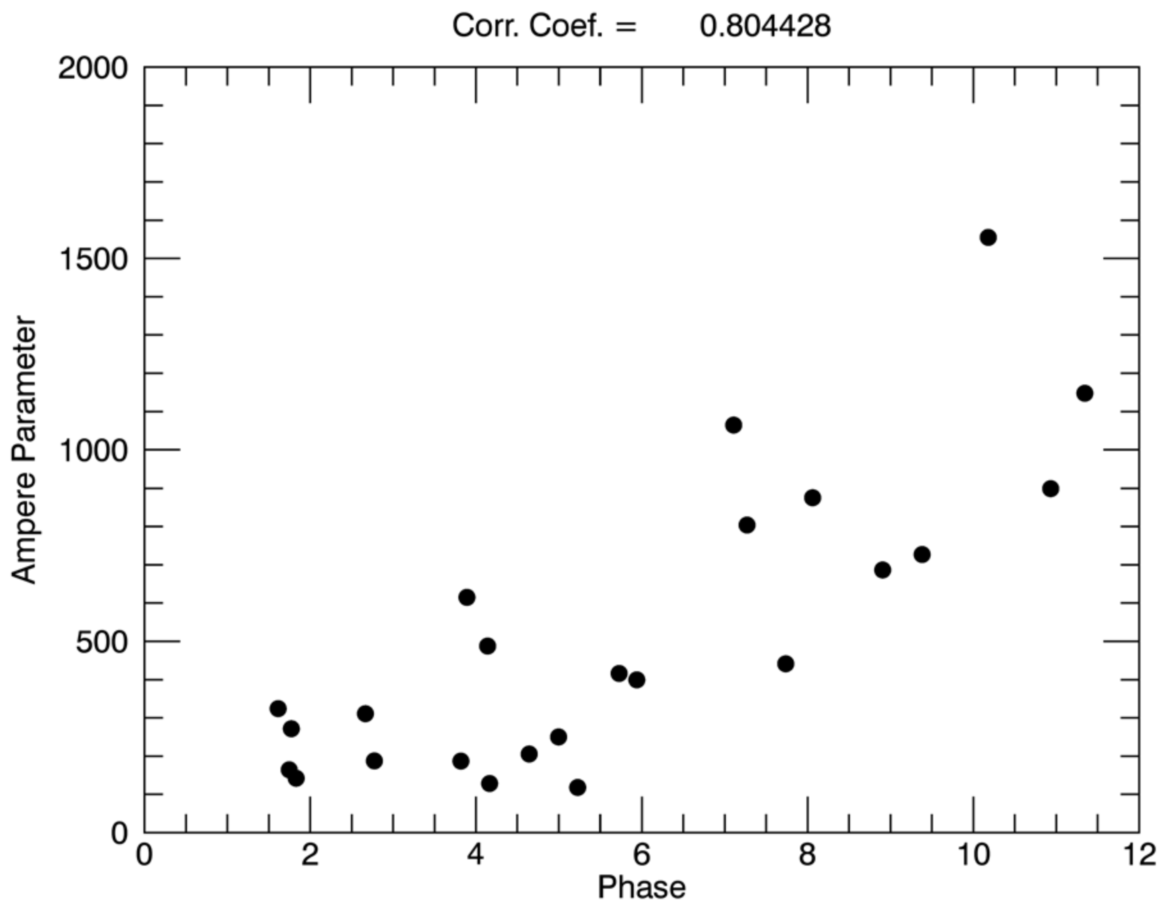

20151220

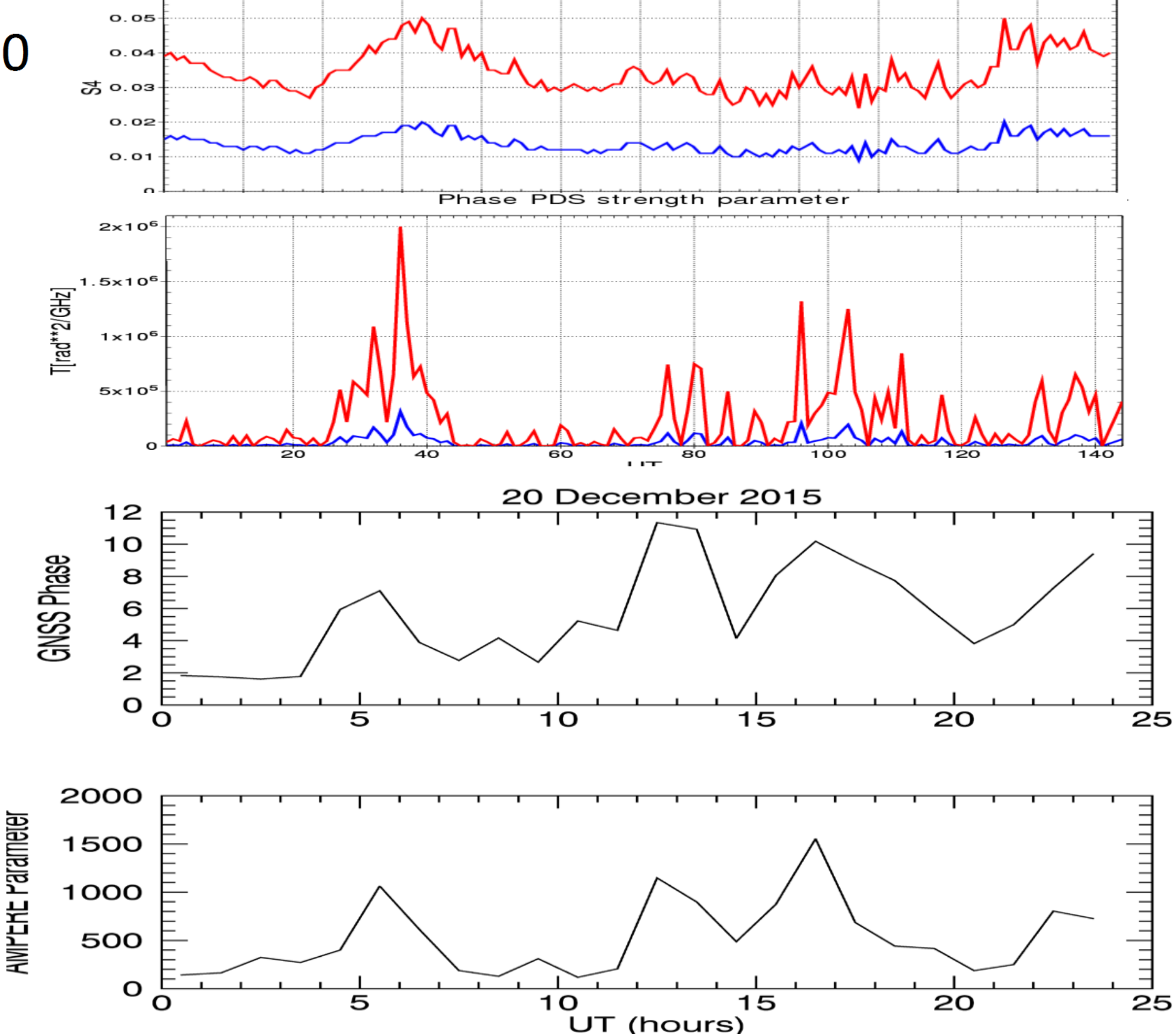
S4
0.05
0.04
0.03
0.02
0.01
Phase PDS strength parameter
T[rad**2/GHz]
2x10⁶
1.5x10⁶
1x10⁶
5x10⁵
0
20
40
60
80
100
120
140
20 December 2015
GNSS Phase
12
10
8
6
4
2
0
5
10
15
20
25
AMPERE Parameter
2000
1500
1000
500
UT (hours)

December 31, 2015 GNSS phase compared to E-north times shear in E-north

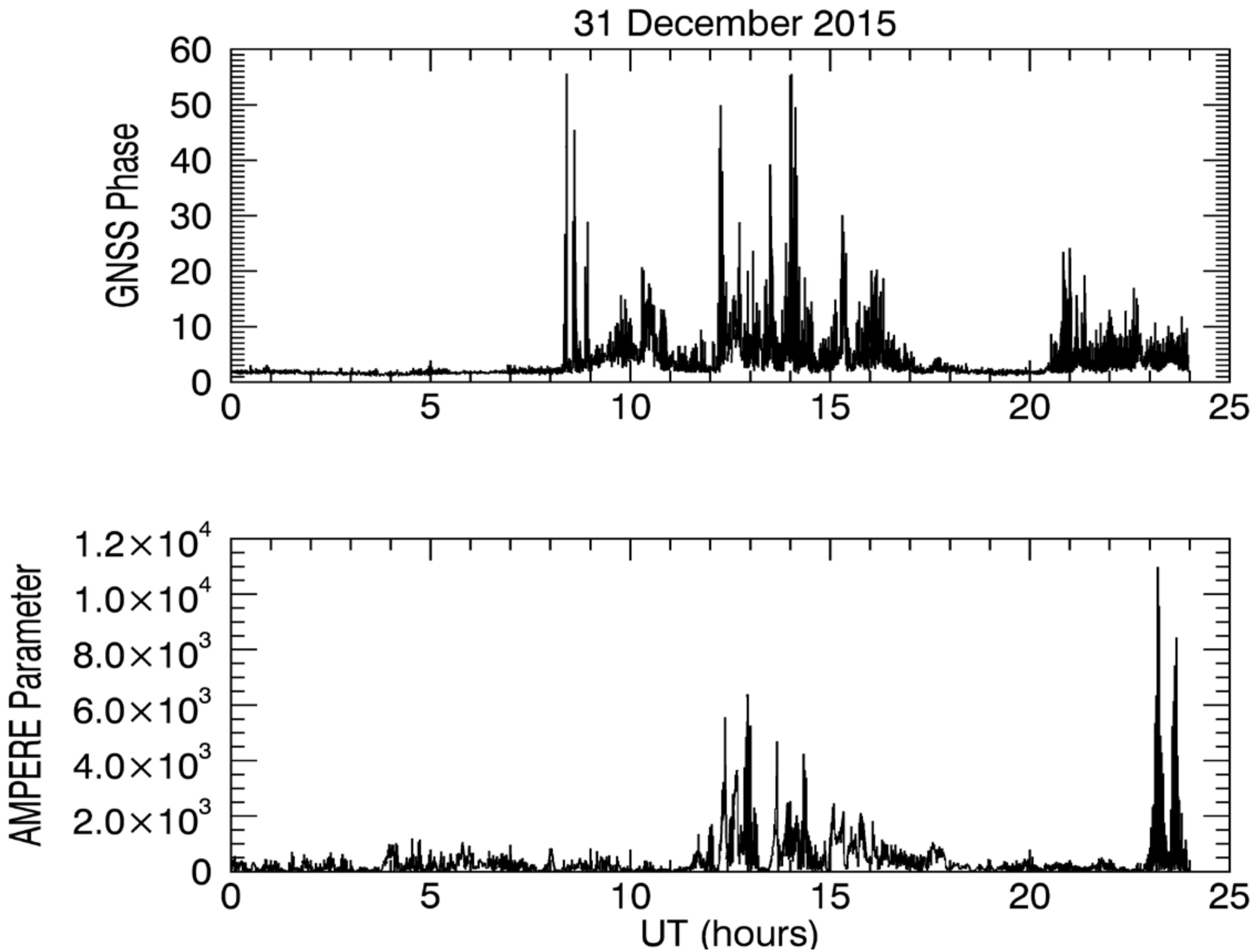

December 31, 2015 GNSS phase compared to E-north times shear in E-north

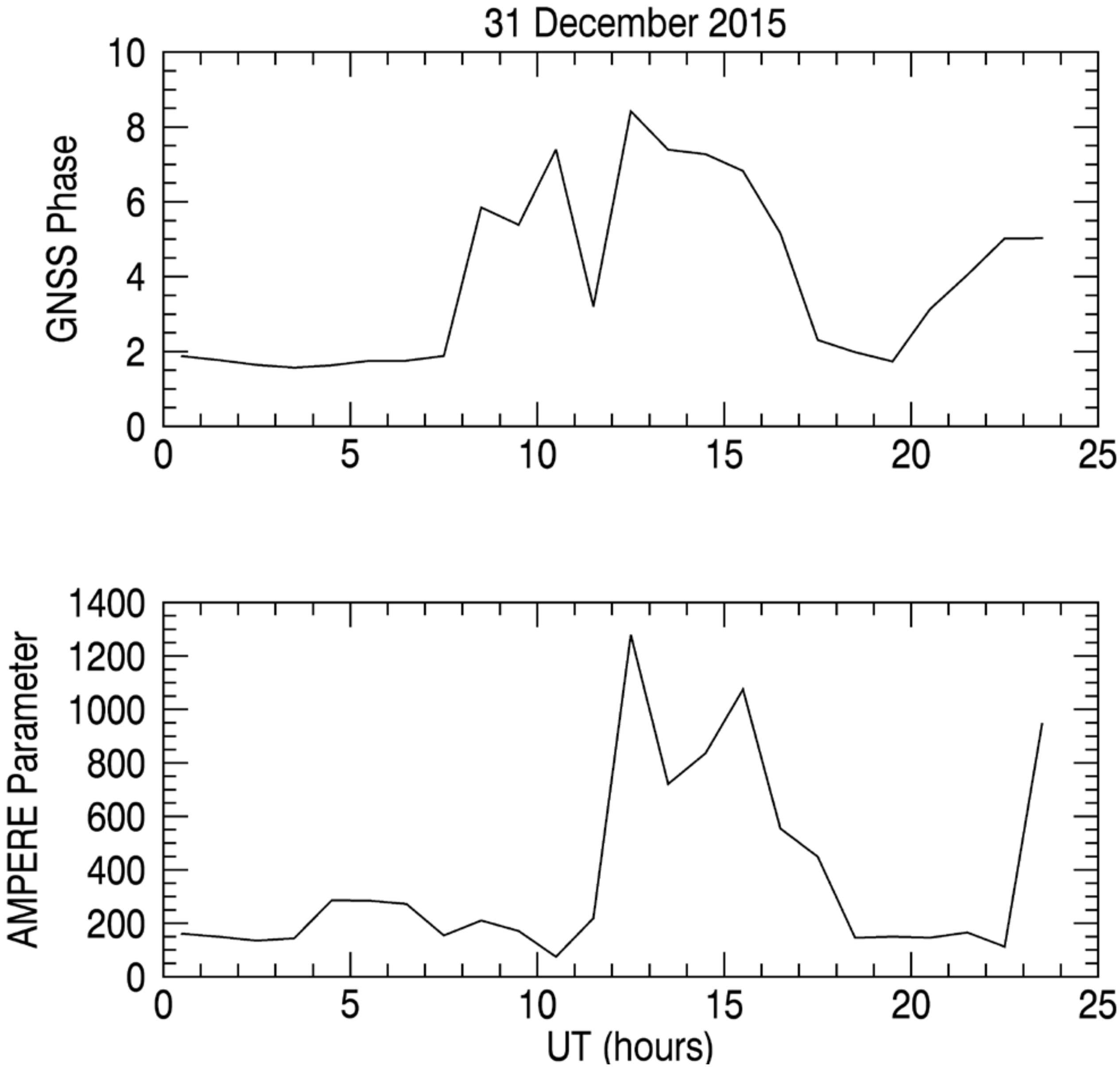

December 31, 2015 GNSS phase compared to E-north times shear in E-north

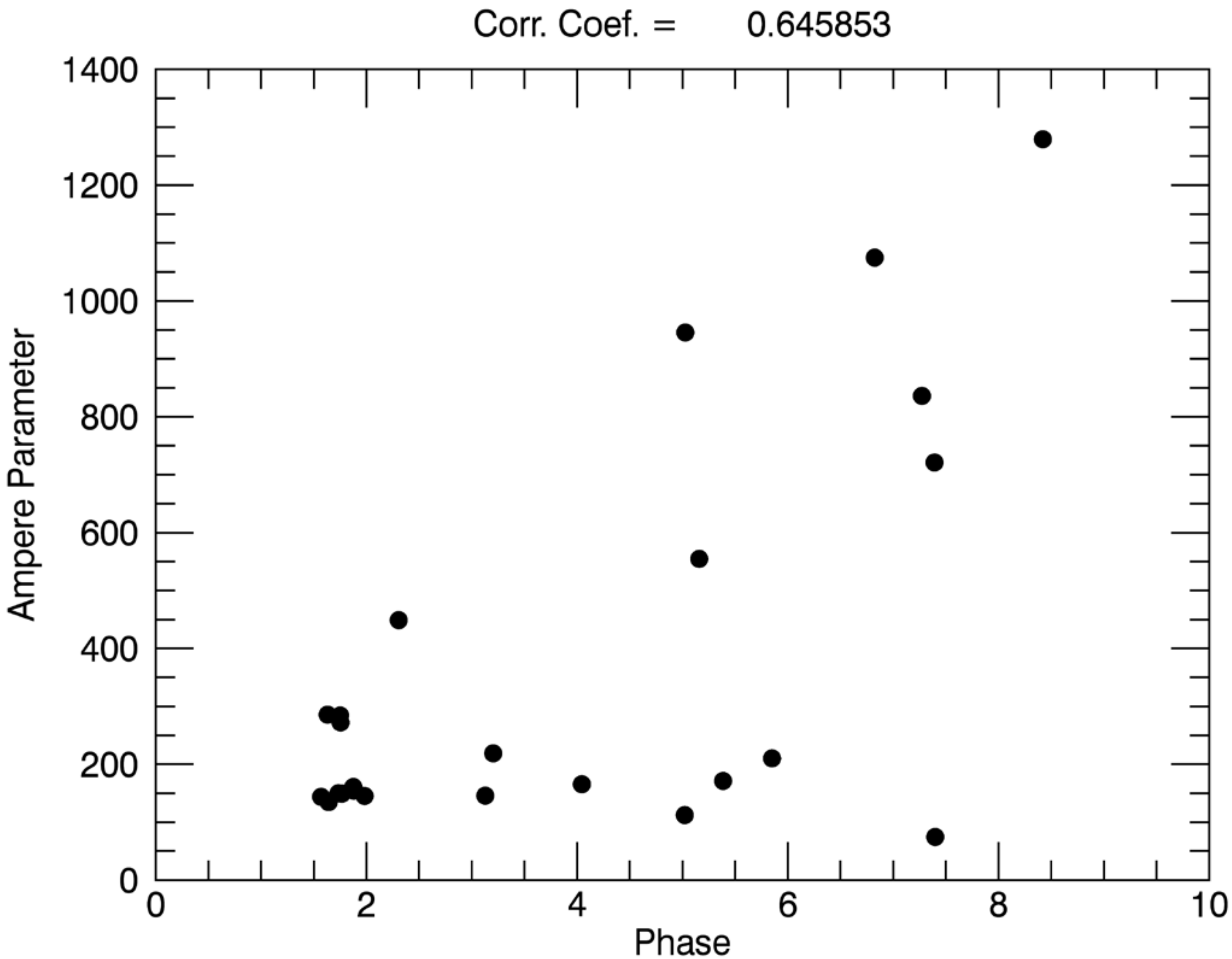

20151231

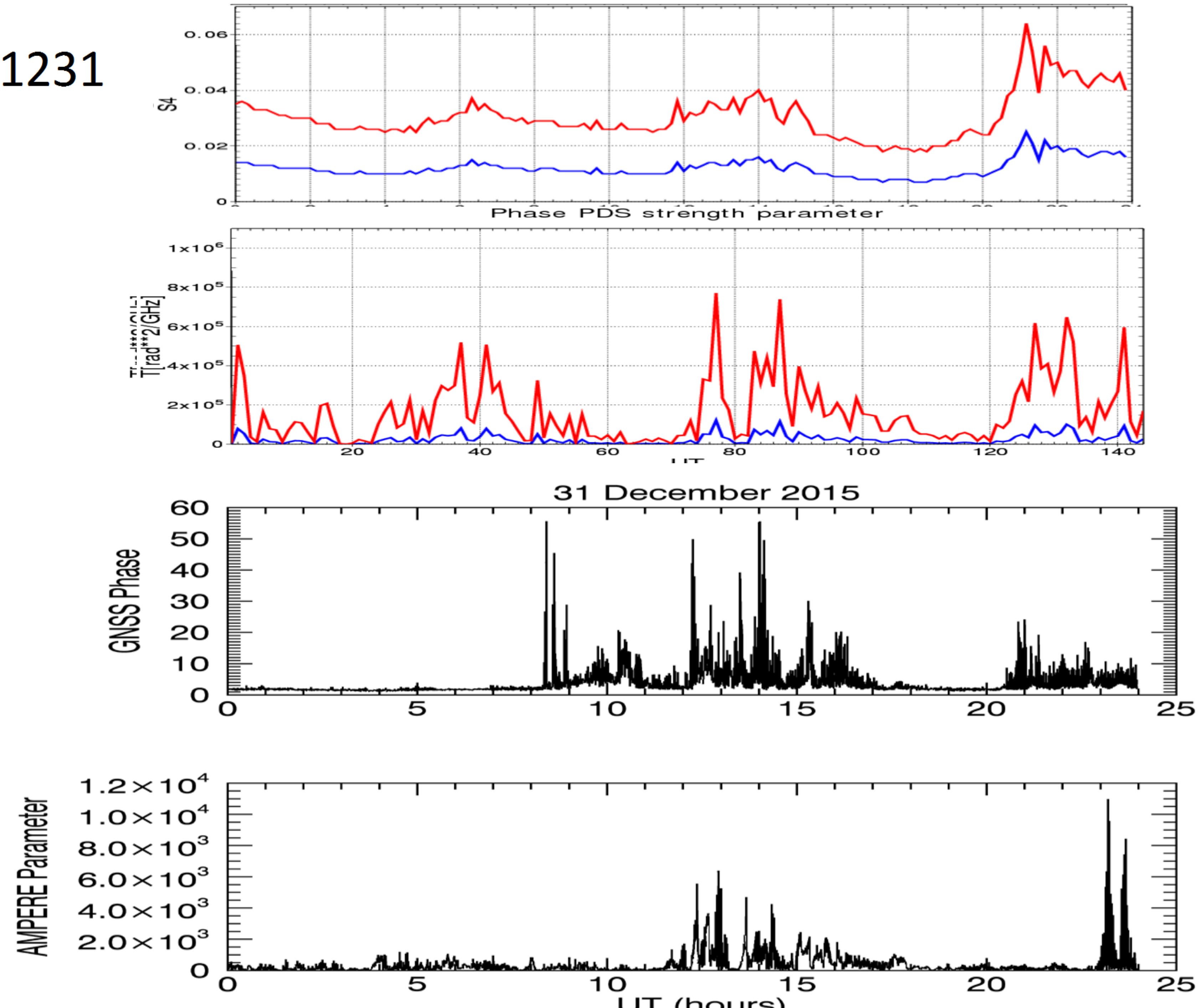

S4
0.06
0.04
0.02
0
Phase PDS strength parameter
T[rad**2/GHz]
1x10⁶
8x10⁵
6x10⁵
4x10⁵
2x10⁵
0
20
40
60
80
100
120
140
31 December 2015
GNSS Phase
60
50
40
30
20
10
0
0
5
10
15
20
25
AMPERE Parameter
1.2×10⁴
1.0×10⁴
8.0×10³
6.0×10³
4.0×10³
2.0×10³
0
0
5
10
15
20
25
UT (hours)

Correlation Coefficients

AMPERE Parameter	20-Dec-15	31-Dec-15
E-north	0.725	0.331
dEn	0.604	0.687
En*dEn	0.804	0.646
E-east	0.279	0.416
dEe	0.386	0.695
J-north	0.604	0.604
dJn	0.478	0.775
J-east	0.001	0.687
dJe	0.376	0.601
E-flux	-0.092	0.536
dEf	0.058	0.539
Joule Heat	0.624	0.637
dJH	0.656	0.716

20151231   6.00000

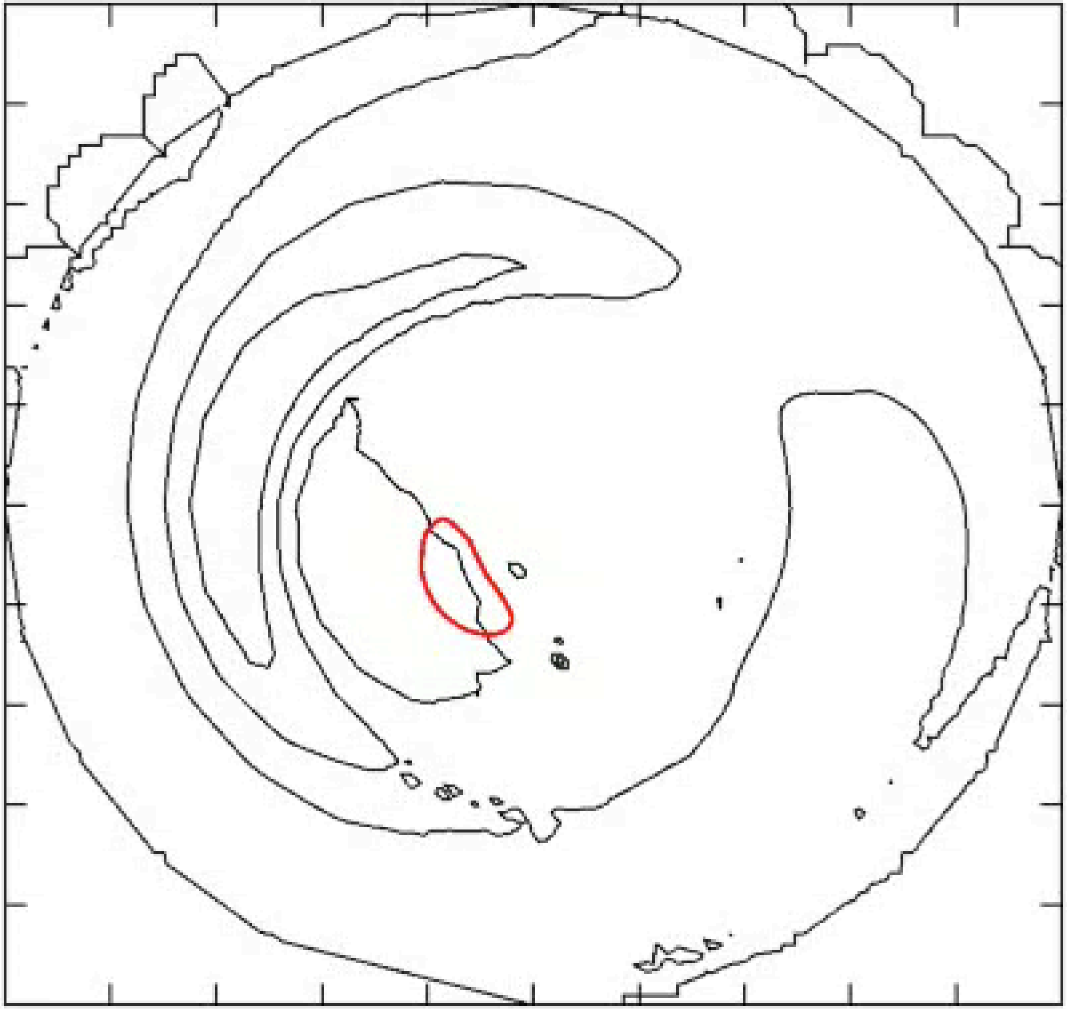

20151220   12.0000

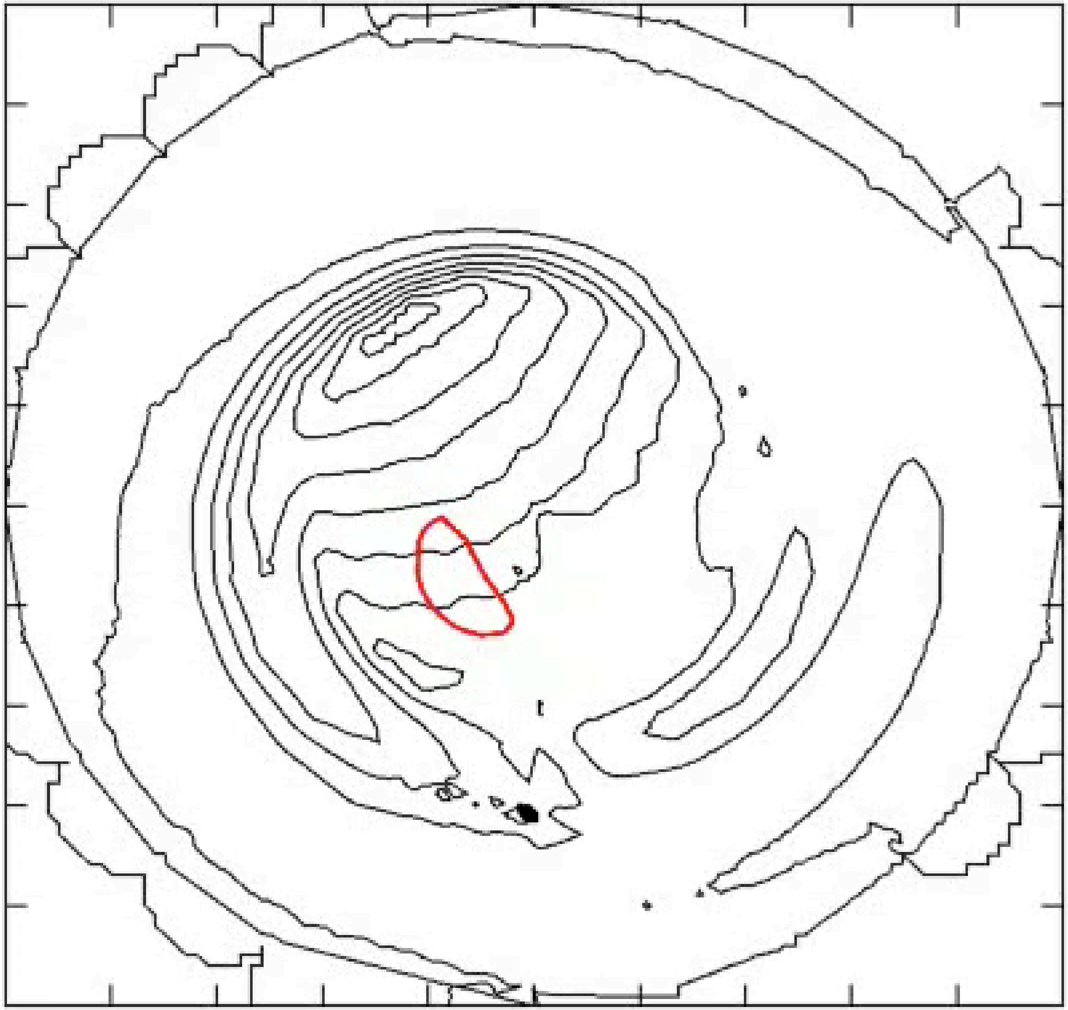

20 December 2015

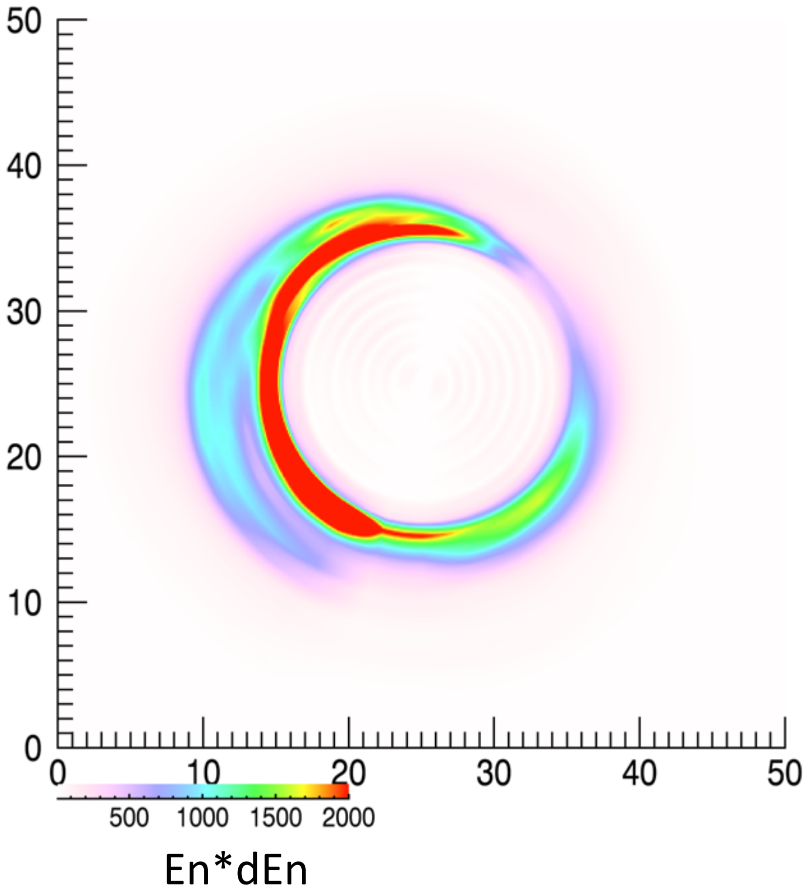

31 December 2015

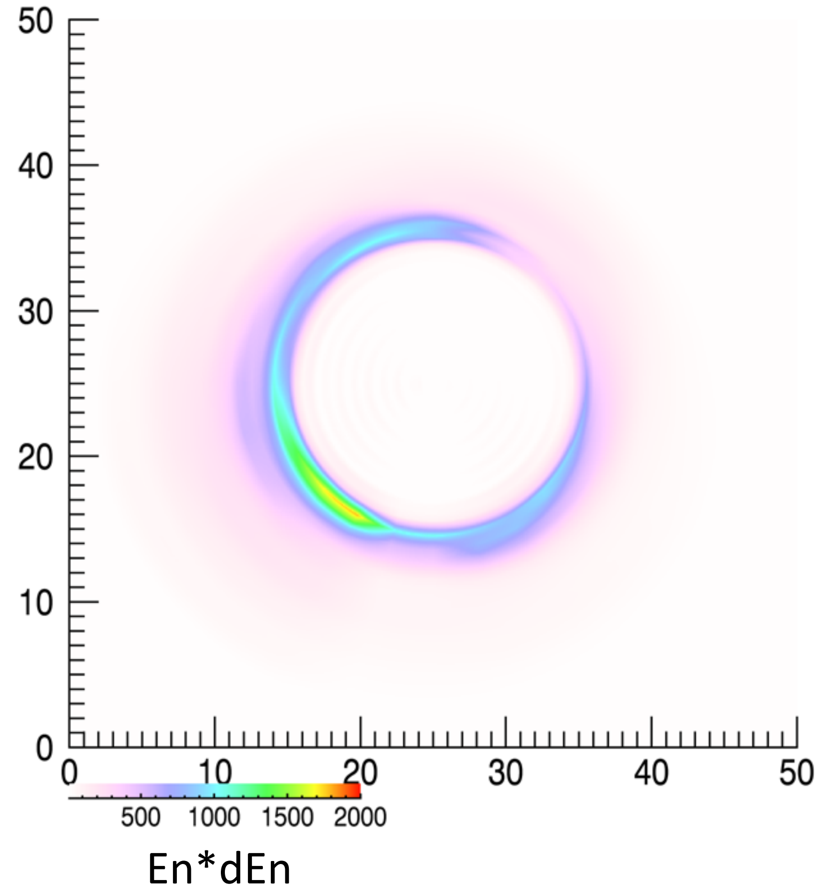

Conclusions

- Phase disturbances measured by Poker Flat GNSS receivers generally correlate with the local gradient in the northward electric field
- The best correlation is with the product of the northward field and the gradient in the northward field
- Correlation is in part consistent with the motion and distortion of drifting plasma patches from the polar cap
- The observed phase disturbances agree with WBMOD climatology that includes geometric enhancement effects
- Electrodynamic parameters derived from global AMPERE measurements of field-aligned currents can be used to predict the occurrence of phase disturbances